EurJIC
European Journal of Inorganic Chemistry

ChemPubSoc Europe

FULL PAPER

DOI:10.1002/ejic.201500632

Affecting the Catalytic Activity of the Known $[Ru(tpy)(bpy)(OH_2)]^{2+}$ Complex in Water Oxidation by Utilization of a Hangman Ligand

Pierre Wrzolek[a] and Matthias Schwalbe*[a]

Keywords: Oxidation / Hydrogen bonds / Ruthenium / N ligands

$[Ru(tpy)(bpy)(OH_2)]^{2+}$ (bpy = 2,2′-bipyridine, tpy = 2,2′;6′,2′′-terpyridine) is the archetype of many known single-site ruthenium complexes used for catalytic water oxidation. Its efficiency is likely influenced by installing a proton-donor/acceptor functionality in proximity to the catalytic site because the reaction mechanism is believed to occur by nucleophilic attack of a water molecule on a high-valent metal–oxo species assisted by hydrogen-bonding interactions. We present herein the results of a study of a new metal complex based on the "hangman" motif that possesses a carboxylic functional group close to the ruhenium center. This catalyst was synthesized in very good yield and fully characterized. We discovered that its catalytic activity was in fact hampered by the presence of the functional group. Further investigations revealed a strong dependence of the catalytic performance not only on the solvent, but also on the counter ion and other additives used.

Introduction

Major fuel sources for the world's energy supply are carbon-based (gas, oil, coal), which emit climate-damaging carbon dioxide when burned. Therefore the search for renewable energy systems to avoid further accumulation of CO_2 in the atmosphere is crucial. One solution to the energy problem is the development of clean and sustainable fuel technologies, for example, the splitting of water into hydrogen and dioxygen to drive a hydrogen-based society.[1] The oxidation of water into protons and dioxygen by a proton-coupled electron transfer (PCET) is the critical, high-energetic, half-reaction of this process. The use of sunlight could assist this transformation and, as a result, the energy of the sun could be stored as chemical bond energy (i.e., artificial photosynthesis).[2] To develop artificial catalysts and mimic the biological process of water splitting, we have to understand the elementary steps that occur at the reaction center in detail. A number of molecular mono- and multinuclear water oxidation catalysts (WOCs) have been reported, but the mechanism of the O–O bond formation remains controversial.[2,3] Ruthenium catalysts have proved to be the best catalytic systems with outstanding activities in terms of high turnover numbers (TONs) and turnover frequencies (TOFs): Sun and co-workers introduced a catalyst containing a bda ligand (bda = 2,2′-bipyridine-6,6′-dicarboxylate) with TONs of up to 55400 and a TOF of 286 s^{-1}.[4]

$[Ru(tpy)(bpy)(OH_2)]^{2+}$ was one of the first single-site catalysts to be studied and has already been well characterized and investigated.[5] Earlier studies suggested that a base-assisted nucleophilic attack of water on a ruthenium–oxo species is the crucial step in O–O bond formation.[6] In fact, the rate-limiting step is the attack of a water molecule on a $[Ru^V{=}O]^{3+}$ species with concomitant loss of a proton.[7] On this basis, we investigated whether this class of complexes would show improved catalytic activity when using the so-called hangman motif. The hangman motif has already demonstrated a positive influence on the H_2O_2 dismutation reaction as well as on the oxygen reduction reaction (ORR) when hangman porphyrins were employed.[8] The oxygen evolution reaction (OER) is the reverse process of the ORR. Hence a proton-donor/acceptor functionality should in principle also support the formation of the O–O bond. The idea is that the attacking water molecule is held in the secondary coordination sphere through a hydrogen-bonding interaction with the functional group, for example, a carboxylic acid, to allow a more efficient O–O bond formation event to take place (see Figure 1).

We modified the tpy unit of the rather simple WOC $[Ru(tpy)(bpy)(OH_2)]^{2+}$ as it has been shown before that substituents on the tpy unit have no significant influence on catalytic performance.[5b] Thus, we report herein the synthesis of a hangman ligand with a carboxylic acid as well as a tpy function on a xanthene backbone that can be used for the creation of ruthenium complexes. The carboxylic acid group can serve just as a hydrogen-bonding partner or can take part in the reaction as proton-donor/acceptor. We

---

[a] Institut für Chemie, Humboldt-Universität zu Berlin,
Brook-Taylor-Str. 2, 12489 Berlin, Germany
E-mail: matthias.schwalbe@hu-berlin.de
https://www.chemie.hu-berlin.de/aglimberg/mschwalbe/index.html

Supporting information for this article is available on the WWW under http://dx.doi.org/10.1002/ejic.201500632.

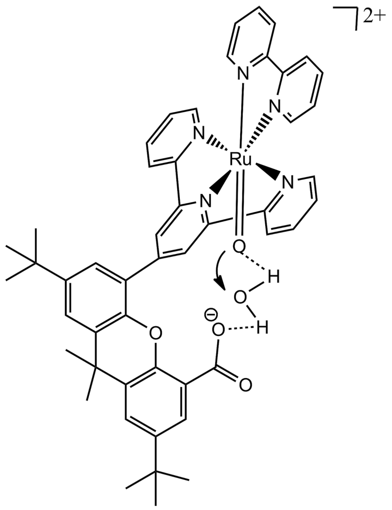

Figure 1. Proposed hydrogen-bonding network with a water molecule held in position for attack on the ruthenium(V)–oxo species.

also replaced the common aqua ligand at the ruthenium center with a labile iodide ligand, which can be easily replaced by water. Synthetically, we were unfortunately not able to isolate a clean ruthenium aqua complex (complex **P2**-H_2O, Scheme 1). However, in earlier work it was shown that similar catalysts for water oxidation with an iodide ligand instead of an aqua ligand also possess high catalytic activity.[9] The mononuclear hangman complexes indeed act as catalysts for chemically driven water oxidation using cerium(IV) ammonium nitrate (CAN) as oxidant. We have further investigated the influence of the axial ligand L as well as the counter anion (Scheme 1) in detail.

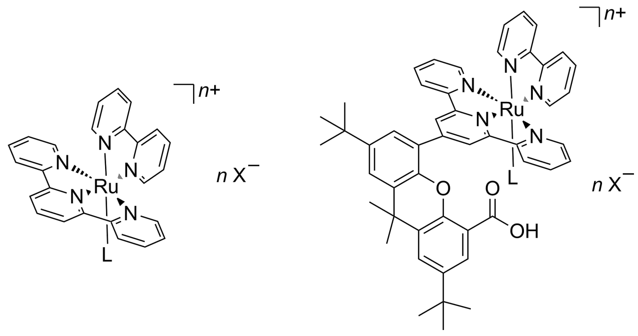

P1-L-X: L = Cl, I ($n = 1$)
H_2O, MeCN ($n = 2$)

X = PF_6, ClO_4

P2-L-X: L = Cl, I ($n = 1$)
H_2O, MeCN ($n = 2$)

X = PF_6, ClO_4

Scheme 1. Ruthenium complexes investigated in this work.

Results

Syntheses and Characterization

$[Ru(tpy)(bpy)Cl]^{2+}$ (**P1**-Cl) was synthesized following a published procedure by the reaction of $RuCl_3 \cdot 3H_2O$ in a two-step reaction with 2,2′;6′,2′′-terpyridine (tpy) and 2,2′-bipyridine (bpy).[10] As the chloride ligand is replaced only slowly by water during the catalytic reaction,[4,9] we also prepared reference complexes with an aqua (**P1**-H_2O) or iodide (**P1**-I) ligand for easier comparison.[5b,9] The xanthene backbone precursor (5-bromo-4-methoxycarbonyl-2,7-di-*tert*-butyl-9,9-dimethylxanthene) was synthesized following the well-described procedure reported earlier by Nocera and co-workers.[11] The desired hangman ligand was obtained after Pd-catalyzed cross-coupling reaction with 4′-dioxoborolatoterpyridine (Figure 2) by using $[Pd(dppf)Cl_2]$ as catalyst, dmso as solvent, and Na_2CO_3 as base in good yield (53% over two steps; further details can be found in the Supporting Information).

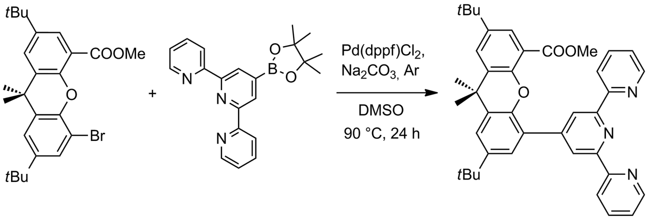

Figure 2. Synthesis of the hangman ligand by Pd-catalyzed cross-coupling reaction of 4′-dioxoborolatoterpyridine and the backbone precursor.

Ruthenium complexation was achieved by using $[Ru(bpy)(Cl)_2(MeCN)_2]$[12] at reflux in dmf. Subsequent ester hydrolysis yielded the new hangman ruthenium complex **P2**-Cl. The exchange of the chloride ligand by an aqua ligand was attempted by reaction with $AgNO_3$ or $AgPF_6$ in mixtures of water with acetone, ethanol, acetonitrile, and 2,2,2-trifluoroethanol (tfe). Unfortunately, we could not obtain a pure product with an aqua ligand in the hangman ruthenium complex in any case. However, after work-up of the attempted synthesis in acetonitrile, a side-product was isolated in the form of an acetonitrile molecule bound to the ruthenium center as the axial ligand (**P2**-MeCN). The procedure followed to obtain this side-product can be found in the Supporting Information.

Because of the problems in isolating a ruthenium aqua complex, we decided to replace the chloride ligand with an iodide ligand. Compound **P2**-**I** was formed in excellent yield (98%) if a mixture of **P2**-Cl in acetone/water (3:4) with 30 equiv. of potassium iodide was heated at reflux overnight. Anion exchange was achieved by treating the initial aqueous solution with either NH_4PF_6 or $NaClO_4$ to form the ionic products **P2**-**I**-PF_6 or **P2**-**I**-ClO_4, respectively.

The purity of all the new complexes was investigated by ^1H NMR spectroscopy and ESI-MS (see the Supporting Information). In the ^1H NMR spectra the axial ligand L has a clear influence on the chemical shifts of the protons in the bipyridine and terpyridine ligands. The most significant shift can be observed for the proton located at the 6-position of the bpy ligand, which is close to the axial ligand. This highly downfield-shifted signal appears at δ = 10.3 ppm for **P2**-Cl, at δ = 10.8 ppm for **P2**-**I**, and at δ = 9.7 ppm for **P2**-MeCN in CD_2Cl_2 as solvent. The other signals of the tpy and bpy ligands are subject to smaller shifts and no changes are observed in the signals of the aliphatic groups on the xanthene backbone (δ = 1.79 ppm for the methyl groups, δ = 1.44 and 1.33 ppm for the *tert*-butyl groups). The anion (PF_6^- or ClO_4^-) has only a minor influence on the chemical shift of the proton signals (<0.1 ppm difference).

UV/Vis absorption spectroscopy revealed that there is hardly any difference in the UV/Vis spectra of **P1**-I-PF_6 and **P2**-I-PF_6 (see Figure S1 in the Supporting Information), which indicates that the hangman functionality has a negligible influence on the electronic properties of the ruthenium center. (This fact is further supported by the electrochemical analysis, see below.) The axial ligand L, however, causes a strong redshift of the metal-to-ligand charge transfer (MLCT) absorption on changing the MeCN ligand (465 nm) to iodide (501 nm) or chloride (509 nm; see Table 1 and Figure S2). Again, the counter ion has a negligible influence on the spectroscopic properties.

Table 1. UV/Vis spectroscopic data for the ruthenium complexes discussed in this work.[a]

Compound	λ_{max} [nm] (ε [$mM^{-1}\,cm^{-1}$])		
P2-MeCN-PF_6	286 (48.3)	309 (33.0)	465 (10.4)
P1-I-PF_6	293 (41.1)	314 (34.4)	501 (10.4)
P2-I-PF_6	294 (40.9)	314 (34.2)	501 (10.4)
P1-Cl-PF_6[b]	281 (33.7)	316 (34.6)	508 (10.7)
P2-Cl-PF_6	284 (44.1)	316 (26.0)	509 (10.2)

[a] Spectra recorded in dcm. [b] From ref.[13]

Cyclovoltammetry was used to determine the electrochemical characteristics of the ruthenium complexes in acetonitrile. Complexes **P1**-I and **P2**-I show basically the same cyclovoltammograms (Figure 3 and Table 2) with a reversible redox event assigned to the Ru^{II}/Ru^{III} couple at 0.45 V versus Fc^+/Fc and an irreversible event assigned to ligand reduction at around –2.0 V. Thus, the hangman functionality does not influence the electronic properties of the [Ru(tpy)(bpy)] unit. These results are in agreement with the measurements carried out by others, which also revealed a mere 60 mV lower oxidation potential of **P1**-Cl compared with **P1**-I.[9,14] On the other hand, the CV data for complex **P2**-MeCN-PF_6 clearly shows the influence of the axial ligand L, because the Ru^{II}/Ru^{III} couple is shifted to higher potentials by around 450 mV (0.89 vs. 0.45 V for **P2**-I-ClO_4). Furthermore, two reversible reduction potentials can be observed at –2.00 and –1.74 V versus Fc^+/Fc as well as one irreversible reduction at around –2.33 V (Figure 3).

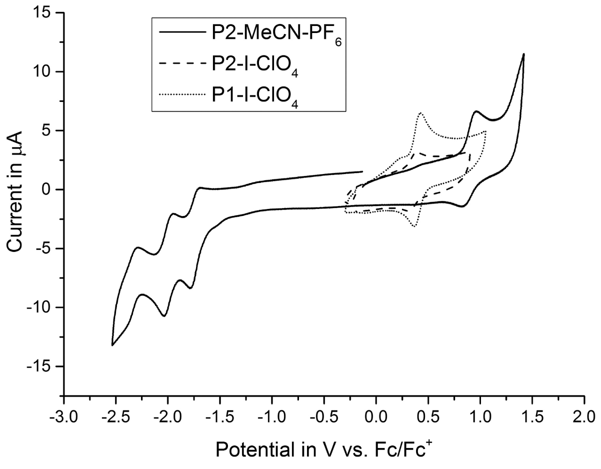

Figure 3. Cyclovoltammograms of **P2**-MeCN-PF_6 (solid line), **P2**-I-ClO_4 (dashed line), and **P1**-I-ClO_4 (dotted line) in acetonitrile obtained with a scan rate of 100 $mV\,s^{-1}$, 0.1 M $TBAPF_6$ as electrolyte, a glassy carbon working electrode, Ag/$AgNO_3$ reference electrode, and Pt wire counter electrode.

Table 2. Cyclovoltammetric data for the ruthenium complexes discussed in this work.[a]

Compound	$E_{1/2}$ [V]				
P1-MeCN-PF_6[b]		ca. –2.00[c]			0.96
P2-MeCN-PF_6	–2.33[c]	ca. –2.00	–1.74		0.89
P1-I-ClO_4		ca. –2.00[c]		0.44	
P2-I-ClO_4		ca. –2.00[c]		0.45	

[a] Data obtained vs. Fc^+/Fc in CH_3CN with 0.1 M $TBAPF_6$ as electrolyte. [b] From ref.[15] [c] Irreversible and cathodic peak potential quoted.

Water Oxidation Catalysis

In this work we were particularly interested in evaluating the catalytic performance of a series of Ru catalysts in water oxidation. The presumed mechanism of water oxidation suggests that base-assisted hydrogen-bonding interactions support O–O bond formation during the attack of a second water molecule on a Ru^V=O species.[5c] Thus, a carboxylic acid functional group is supposed to accelerate the formation of the Ru^{III}–OOH intermediate, which is further oxidized by a sacrificial electron acceptor to yield a peroxide species before dioxygen is finally released.

Dioxygen evolution experiments were carried out by using a custom-built apparatus consisting of a 7 mL reaction vessel equipped with a septum (see Figure S6 in the Supporting Information). The apparatus was kept at a constant temperature of 20 °C for the duration of the experiment and the O_2 concentration in the headspace was monitored every second with an optical probe (Unisense Micro-Optode Meter). Then 2 mL of a deaerated solution of $(NH_4)_2[Ce(NO_3)_6]$ (CAN; 100 equiv.) in 1 M HNO_3 containing an indicated amount of additive was injected through the rubber septum resulting in a final catalyst concentration of 1×10^{-3} M. The solution was stirred for the entire reaction. We had to use tfe or Triton X-100® (see Figure S15) as an additive because of the very low solubility of compounds **P2**-L in pure water.

Initial experiments were conducted to determine the catalytic activity of **P1**-I in comparison with that of **P2**-I by using 5% tfe as additive (Figure 4). After a solution of CAN in HNO_3 and tfe (or Triton X-100®) was added to the complex(es), oxygen was instantly liberated. The headspace over the solution after the reaction had ceased was also analyzed by gas chromatography and revealed the sole formation of dioxygen. We used 100 equiv. of CAN and thus the TONs were limited to a maximum of 25. The reference experiment with compound **P1**-I-ClO$_4$ produced O$_2$ with a TON of 22.5 after 1 h, practically maintaining an oxidative efficiency of 90 %, which had also been observed previously.[9] In the case of compound **P2**-I-ClO$_4$, a TON of 21.5 was obtained after 8 h, reaching an oxidation efficiency of 86 % (although the reaction was not finished at that point and a very slow increase in O$_2$ concentration was still observed). Thus, surprisingly, the hangman complex **P2**-I-ClO$_4$ was much slower than the reference complex **P1**-I-ClO$_4$. Although **P1**-I-ClO$_4$ shows the expected water oxidation efficiency[9] with the release of O$_2$ leveling off after 45 min, the hangman complex started to slowly level off only after 6 hours and the reaction was not finished after 18 hours of reaction time. In a blank experiment without the catalyst but otherwise identical conditions we found that no or only a negligible amount of O$_2$ formed in the same time period. These results are summarized and discussed below through a comparison of the maximum TOF values (see Figures S8 and S9 and Table S1 in the Supporting Information) obtained by plotting the TOF values versus time.

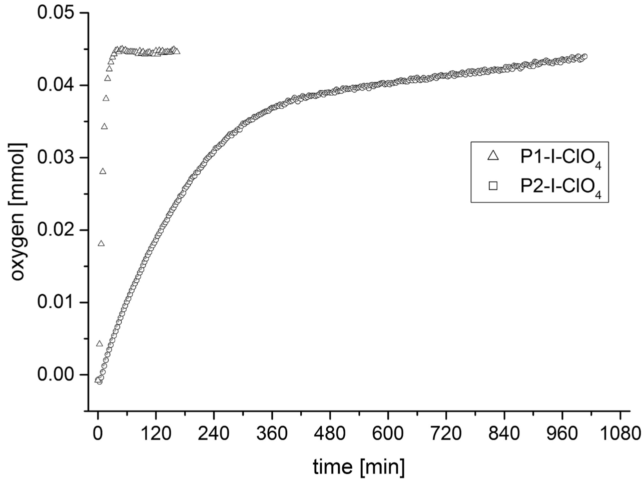

Figure 4. Oxygen evolution traces of **P1**-I-ClO$_4$ and **P2**-I-ClO$_4$ vs. time [conditions: 1 M HNO$_3$ aqueous solution with 5 % tfe (2 mL) containing CAN (100 equiv.) and the catalyst (1×10^{-3} M)].

We also investigated the influence of different amounts of additives on the catalytic reaction and added tfe and Triton X-100® in different quantities to increase the solubility of compounds **P2**-I-ClO$_4$ and **P2**-I-PF$_6$ in aqueous solution. We found that the additives were optimal for only one counter ion, either PF$_6^-$ or ClO$_4^-$ (see Figure S5 in the Supporting Information). Other additives, such as acetonitrile, tetrahydrofuran, and dimethylformamide, resulted in no or very low catalytic activity. The use of tfe in combination with **P2**-I-ClO$_4$ led to especially good results. Without the addition of tfe, **P2**-I-ClO$_4$ was not soluble in water and hence showed no catalytic activity (Table 3). With 5 % tfe in water, the ruthenium complex dissolved completely and we obtained the highest catalytic activity, approaching the TON value of the parent compound **P1**-I-ClO$_4$. Further addition of tfe, to 10 or 20 % tfe, decreased the catalytic activity rapidly (Table 3 and Figures S7 and S8). Under the same catalytic conditions as employed for **P2**-I-ClO$_4$, the use of compound **P2**-I-PF$_6$ did not lead to the formation of any dioxygen. However, on addition of Triton X-100® instead of tfe, oxygen was obtained with a maximum TON of 11 with 1 % Triton X-100® in water (Table 4); no CO$_2$ was detected by GC after the reaction was finished. However, the amount of oxygen produced was far less than that produced with **P2**-I-ClO$_4$ under the optimized conditions. Interestingly, a TON of only 2 was obtained with **P2**-I-ClO$_4$ using 1 % Triton X-100®, much lower than the TONs obtained with tfe as additive.

Table 3. TON determined after 8 h and maximum TOF values obtained for catalytic water oxidation with **P2**-I-ClO$_4$ in a mixture of water and tfe.

tfe [%]	TON	TOF$_{max}$ [min^{-1}] (time [min])
0	0	0
5	21.5	0.085 (42)
10	19	0.078 (81)
20	11	0.038 (90)

Table 4. TON determined after 8 h and maximum TOF values obtained for catalytic water oxidation with **P2**-I-PF$_6$ in a mixture of water and Triton X-100®.

Triton X-100® [%]	TON	TOF$_{max}$ [min^{-1}] (time [min])
0	0	0
1	11	0.0314 (48)
5	1	0.0036 (70)

In summary, the highest catalytic activity was obtained with the solvent mixture of 5 % tfe in water and perchlorate as the counter ion. The achieved TON of 21.5 (determined after 8 h) for **P2**-I-ClO$_4$ is only slightly lower than the TON of 22.5 (determined after 45 min) of the reference complex **P1**-I-ClO$_4$. The significant difference is found in the TOF: The reference complex **P1**-I-ClO$_4$ has a maximum TOF of 1.41 min^{-1} (reached after 9 min, see Figure S9 in the Supporting Information), whereas the catalytic activity of the hangman complex **P2**-I-ClO$_4$ is considerably lower with a maximum TOF of 0.085 min^{-1} (reached after 50 min, see Figure S8).

One of the reasons for the low catalytic activity might be the interaction between the complex and the additive(s). The highly oxidizing environment probably leads to decomposition (oxidation) of the additive and therefore a decrease in dioxygen evolution. This possibility is supported by the fact that the catalytic activity decreases as the amount of additive increases. Another strong influence is the mismatched pH of the solution: A deprotonated acid group should support the hangman effect in the O–O bond formation step; however, this second coordination sphere effect cannot occur with a mismatched pH of around 1, which is needed to work with CAN in our experiments, because at this pH the acid group is still protonated (we assume a pK_a value of around 4, similar to benzoic acid) and cannot support the attack of the second water molecule on the ruthenium–oxo moiety. A similar effect could be observed in water oxidation catalysis with iron complexes investigated by Yang and co-workers.[16] Unfortunately, we could not find suitable reaction conditions comprising higher pH values; the use of periodate as sacrificial electron acceptor, for example, did not lead to oxygen formation.

Another problem could be the hydrogen-bonding interaction presented in Figure 1, which might actually result in the fixation of reactive oxygen species immediately after the formation of the O–O bond at the reaction center. In the end, this interaction might decelerate the release of dioxygen and open up alternative pathways that lead to side-reactions, for example, oxidation of the additive or decomposition of the catalyst. However, we conducted an experiment in which we added a further 100 equiv. of CAN to the reaction solution; this led to further evolution of dioxygen at a similar rate to that observed in the first run (see Figure S10 in Supporting Information), which proved the catalyst to be fairly stable.

After the reaction was finished, the headspace of the reaction vessel was analyzed by gas chromatography and only O_2 and no CO_2 was detected. On the one hand, this further indicates the stability of the catalyst and, on the other hand, shows that decomposition of the additive was not complete; for example, just alcohol (tfe) oxidation to aldehyde or acid took place.

To obtain mechanistic information, the first two steps of the catalytic mechanism were investigated by UV/Vis spectroscopy. The UV/Vis spectral changes observed for **P2-I-**ClO_4 before and after the addition of 2 equivalents of CAN in a two-step reaction in 10% tfe in water are shown in Figures S3 and S4 in the Supporting Information. The absorption maximum at 503 nm corresponding to the MLCT state is diminished in accordance with the formation of a high-valent metal–oxo (or hydroxo) species, as described in the literature.[5c,17] A change in the UV/Vis spectrum after the addition of a third equivalent of CAN could not be observed. Thus, we assume that the first oxidation of catalyst **P2-I-**ClO_4 in aqueous solution will yield a Ru^{III}–OH species and the second oxidation a Ru^{IV}=O species, as described in the literature.[17]

To further investigate the stability of the catalyst, the final reaction solution was neutralized, extracted with chloroform, and the organic phase was washed with brine. After removal of the solvent the resulting residue was analyzed by MS and NMR spectroscopy. The ^1H NMR spectrum was not interpretable because of the overlap of too many signals. No signs of the starting catalyst **P2-I** or ruthenium-containing decomposition products were identified by ESI-MS, probably due to an unsuitable ionization method. Analysis by MALDI-TOF MS showed that the major signal at m/z = 854.2 arises from the deprotonated ruthenium(II) complex without the ligand L ($[C_{49}H_{46}N_5O_3Ru]^+$; see Figure S11 in the Supporting Information). The peak at m/z = 890.3 indicates the inclusion of two water molecules and points to a structure similar to the one shown in Figure 1 in which the axial ligand on the ruthenium is a water molecule and the second water molecule may be hydrogen-bonded to the deprotonated carboxylic acid functionality and the water molecule in the first coordination sphere. The inclusion of the second water molecule could be observed by MALDI-TOF MS and MS/MS fragmentation through a step-wise loss of 2 equivalents of water (see Figure S14). We did not detect any high-valent ruthenium species, probably because of the work-up procedure. These results indicate that the initial catalyst **P2-I** is transformed into the active (aqua) species upon oxidation with CAN and that decomposition of the catalyst is only marginal.

Conclusions

This study has demonstrated the successful synthesis of a hangman analogue of the well-known water oxidation catalyst $[Ru(tpy)(bpy)(OH_2)]^{2+}$.[5c,18] The new hangman complex **P2-I** showed activity in catalytic water oxidation using CAN as oxidant, reaching almost the same overall TON as the parent compound **P1-I** under the optimized conditions. Investigation of various modifications of the reaction conditions showed a strong dependence on the solvent mixture, that is, the nature of additive, as well as on the counter ion. Additives had to be used to solubilize the hangman complexes in 1 M HNO_3, with tfe and Triton X-100® proving most effective; the best results were obtained by using 5% tfe. A strong dependence on the counter ion could also be shown, with perchlorate proving to be optimal for water oxidation catalysis. It is worth noting that the nature of acid used affects the reaction, as revealed in an earlier study (HNO_3 outperformed H_2SO_4, CF_3SO_3H, and $HClO_4$ for different reasons).[19]

The hangman complex **P2-I-**ClO_4 showed a 16-fold slower reaction rate than the parent compound with a maximum TOF of 0.085 min^{-1} compared with 1.41 min^{-1} for **P1-I-**ClO_4 under the same catalytic conditions. This decelerating effect can be attributed to two major effects. On the one hand, the mismatched pH of the solution leaves the hanging carboxylic group protonated and hence does not allow favorable hydrogen-bonding interactions to form during the O–O bond formation, as has recently been observed in iron-catalyzed water oxidation.[16] On the other hand, there could be a stabilizing effect exerted by the protonated carboxylic acid group on the high-valent metal–(hydro)peroxo intermediates that emerge during the catalytic reaction. Hydrogen-bonding interactions seem to stabilize these intermediates in a way such that other side-reactions become more likely, such as additive decomposition. Nevertheless, the ruthenium compound **P2** seems to be stable under the harsh conditions because water oxidation catalysis continues after the addition of a second equivalent of CAN and the ruthenium complex is still observable in MALDI-TOF MS experiments.

In summary, in our investigation hydrogen bonds involving the hanging functional group do not enhance the activity in catalytic water oxidation (very likely due to a mismatch in pH). However, they can potentially be used to stabilize reactive intermediates such that they are available for further spectroscopic characterization, which will be the topic of future work.

Experimental Section

General Considerations: [$RuCl_2(MeCN)_2$] was prepared according to a literature procedure.[20] dmso (99.9+%) was purchased from Aldrich and ceric ammonium nitrate (CAN) was purchased from Acros. All other reagents were purchased from Aldrich Chemical Co. or ABCR and used without further purification. The solvents used were Chromasolve HPLC grade. All the reactions were routinely performed under argon by using standard Schlenk techniques. Work-up was usually performed under standard bench conditions.

The ruthenium compounds were synthesized as described in the following. All analytical data as well as the syntheses of organic compounds (and their numbering) are listed in the Supporting Information.

2,2′-Bipyridyl(chloro)[4-methoxycarbonyl-5-(2,2′;6′,2′′-terpyridin-4′-yl)-2,7-di-*tert*-butyl-9,9-dimethylxanthene]ruthenium(II) Perchlorate (P2Me-Cl-ClO_4): A Schlenk flask was charged with **5** (50 mg, 80 μmol) and [$Ru(bpy)(MeCN)_2Cl_2$] (33 mg, 80 μmol).[20] Upon addition of argon-degassed dimethylformamide (20 mL), the solution was heated at 80 °C for 8 h and then stirred for a further 48 h at room temperature. The solvent was evaporated to give a crude product, which was purified by flash chromatography on aluminium oxide. Impurities were first eluted with ethyl acetate and the product was then obtained by changing the eluent to ethanol and later to $EtOH/H_2O$/satd. aq. KNO_3 (9:1:0.05). The volatiles were removed in vacuo and the product was recrystallized from MeOH/water/$NaClO_4$ to yield **P2**Me-Cl-ClO_4 (76 mg, 90%).

2,2′-Bipyridyl(chloro)[4-hydroxycarbonyl-5-(2,2′;6′,2′′-terpyridin-4′-yl)-2,7-di-*tert*-butyl-9,9-dimethylxanthene]ruthenium(II) Perchlorate (P2-Cl-ClO_4): A 3 M solution of NaOH (2 mL) was added to a stirred solution of **P2**-Me-Cl-ClO_4 (20 mg, 19 μmol) in MeOH (10 mL) and the resulting mixture was heated at reflux for 8 h. The solution was concentrated by rotary evaporation to give a crude product, which was redissolved in 0.5 M HCl (10 mL). The solution was extracted with $CHCl_3$ and the organic phase was washed with water. The solvent was evaporated and the product recrystallized from MeOH/water/$NaClO_4$. **P2**-Cl-ClO_4 was obtained in 90% yield (18 mg).

Synthesis of 2,2′-Bipyridyl(iodo)[4-hydroxycarbonyl-5-(2,2′;6′,2′′-terpyridin-4′-yl)-2,7-di-*tert*-butyl-9,9-dimethylxanthene]ruthenium(II) Perchlorate (P2-I-ClO_4): A mixture of **P2**-Cl-ClO_4 (36 mg, 0.040 mmol) and KI (200 mg, 1.20 mmol) in acetone (3 mL) and water (4 mL) was heated at reflux overnight. $NaClO_4$ (160 mg) was added and the precipitate was collected while it was hot, washed with water, and dried to afford **P2**-I-ClO_4 as a brown powder in 98% yield (43 mg).

Synthesis of Acetonitrile(2,2′-bipyridyl)[4-hydroxycarbonyl-5-(2,2′;6′,2′′-terpyridin-4′-yl)-2,7-di-*tert*-butyl-9,9-dimethylxanthene]ruthenium(II) Perchlorate (P2-MeCN-ClO_4): A mixture of **P2**-I-ClO_4 (50 mg, 0.050 mmol) and $AgNO_3$ (85 mg, 0.50 mmol, 10.0 equiv.) in acetonitrile (3 mL) and water (4 mL) was heated at reflux overnight and filtered. $NaClO_4$ (100 mg) was added and the precipitate was collected while it was hot, washed with water, and dried to afford **P2**-MeCN-ClO_4 as a light-brown powder in 98% yield (49 mg).

Supporting Information (see footnote on the first page of this article): details of the synthesis of the ligand, analytical data of all relevant compounds, UV/Vis spectra, and further catalytic data.

Acknowledgments

The authors are grateful to Unifying Concepts in Catalysis (UniCat), Berlin (grant to P. W.) and to the Deutsche Forschungsgemeinschaft (DFG) (grant SCHW 1454/3-2, to M. S.) for financial support.

---

[1] a) G. A. Olah, *Angew. Chem. Int. Ed.* **2005**, *44*, 2636–2639; b) R. J. Andres, J. S. Gregg, L. Losey, G. Marland, T. A. Boden, *Tellus Ser. B* **2011**, *63*, 309–327; c) N. S. Lewis, D. G. Nocera, *Proc. Natl. Acad. Sci. USA* **2006**, *103*, 15729–15735.

[2] M. D. Kärkäs, O. Verho, E. V. Johnston, B. Åkermark, *Chem. Rev.* **2014**, *114*, 11863–12001.

[3] a) X. Sala, S. Maji, R. Bofill, J. García-Antón, L. Escriche, A. Llobet, *Acc. Chem. Res.* **2014**, *47*, 504–516; b) D. G. H. Hetterscheid, J. N. H. Reek, *Angew. Chem. Int. Ed.* **2012**, *51*, 9740–9747; *Angew. Chem.* **2012**, *124*, 9878; c) P. Du, R. Eisenberg, *Energy Environ. Sci.* **2012**, *5*, 6012–6021.

[4] a) L. Duan, C. M. Araujo, M. S. G. Ahlquist, L. Sun, *Proc. Natl. Acad. Sci. USA* **2012**, *109*, 15584–15588; b) L. Wang, L. Duan, Y. Wang, M. S. G. Ahlquist, L. Sun, *Chem. Commun.* **2014**, *50*, 12947–12950.

[5] a) J. J. Concepcion, J. W. Jurss, J. L. Templeton, T. J. Meyer, *J. Am. Chem. Soc.* **2008**, *130*, 16462–16463; b) D. J. Wasylenko, C. Ganesamoorthy, B. D. Koivisto, M. A. Henderson, C. P. Berlinguette, *Inorg. Chem.* **2010**, *49*, 2202–2209; c) K. J. Takeuchi, M. S. Thompson, D. W. Pipes, T. J. Meyer, *Inorg. Chem.* **1984**, *23*, 1845–1851.

[6] R. A. Binstead, C. W. Chronister, J. Ni, C. M. Hartshorn, T. J. Meyer, *J. Am. Chem. Soc.* **2000**, *122*, 8464–8473.

[7] C. J. Gagliardi, A. K. Vannucci, J. J. Concepcion, Z. Chen, T. J. Meyer, *Energy Environ. Sci.* **2012**, *5*, 7704–7717.

[8] a) L. L. Chng, C. J. Chang, D. G. Nocera, *Org. Lett.* **2003**, *5*, 2421–2424; b) C. J. Chang, L. L. Chng, D. G. Nocera, *J. Am. Chem. Soc.* **2003**, *125*, 1866–1876; c) R. McGuire, D. K. Dogutan, T. S. Teets, J. Suntivich, Y. Shao-Horn, D. G. Nocera, *Chem. Sci.* **2010**, *1*, 411–414.

[9] N. Kaveevivitchai, R. Zong, H.-W. Tseng, R. Chitta, R. P. Thummel, *Inorg. Chem.* **2012**, *51*, 2930–2939.

[10] a) T. Ben Hadda, H. Le Bozec, *Inorg. Chim. Acta* **1993**, *204*, 103–107; b) B. P. Sullivan, J. M. Calvert, T. J. Meyer, *Inorg. Chem.* **1980**, *19*, 1404–1407.

[11] C. J. Chang, C.-Y. Yeh, D. G. Nocera, *J. Org. Chem.* **2002**, *67*, 1403–1406.

[12] a) L. Spiccia, G. B. Deacon, C. M. Kepert, *Coord. Chem. Rev.* **2004**, *248*, 1329–1341; b) D. Mulhern, S. Brooker, H. Gorls, S. Rau, J. G. Vos, *Dalton Trans.* **2006**, 51–57.

[13] H.-W. Tseng, R. Zong, J. T. Muckerman, R. Thummel, *Inorg. Chem.* **2008**, *47*, 11763–11773.

[14] C.-N. Tsai, M. M. Allard, R. L. Lord, D.-W. Luo, Y.-J. Chen, H. B. Schlegel, J. F. Endicott, *Inorg. Chem.* **2011**, *50*, 11965–11977.

[15] E. C. Constable, A. M. W. C. Thompson, *New J. Chem.* **1996**, *20*, 65–82.

[16] W. A. Hoffert, M. T. Mock, A. M. Appel, J. Y. Yang, *Eur. J. Inorg. Chem.* **2013**, 3846–3857.

[17] D. J. Wasylenko, C. Ganesamoorthy, M. A. Henderson, B. D. Koivisto, H. D. Osthoff, C. P. Berlinguette, *J. Am. Chem. Soc.* **2010**, *132*, 16094–16106.

[18] a) T. W. Welch, S. A. Ciftan, P. S. White, H. H. Thorp, *Inorg. Chem.* **1997**, *36*, 4812–4821; b) J. J. Concepcion, J. W. Jurss, M. R. Norris, Z. Chen, J. L. Templeton, T. J. Meyer, *Inorg. Chem.* **2010**, *49*, 1277–1279.

[19] D. J. Wasylenko, C. Ganesamoorthy, M. A. Henderson, C. P. Berlinguette, *Inorg. Chem.* **2011**, *50*, 3662–3672.

[20] D. Mulhern, S. Brooker, H. Gorls, S. Rau, J. G. Vos, *Dalton Trans.* **2006**, 51–57.

Received: June 9, 2015